A Novel Thermothickening Phenomenon Exhibited by a Triblock Polyampholyte in Aqueous Salt-Free Solutions

Frédéric Bossard,[†] Constantinos Tsitsilianis,[*,†,‡] Spyros N. Yannopoulos,[†] Georgios Petekidis,[§] and Vasiliki Sfika[†,‡]

Institute of Chemical Engineering and High-Temperature Chemical Processes—Foundation for Research and Technology (ICE/HT-FORTH), P.O. Box 1414, 26504 Patras, Greece; Department of Chemical Engineering, University of Patras, 26504 Patras, Greece; and Institute of Electronic Structure and Laser, GR-71110 Heraklion, Crete, Greece

Received December 2, 2004; Revised Manuscript Received February 2, 2005

ABSTRACT: A novel thermothickening phenomenon exhibited by a water-soluble triblock copolymer in salt-free aqueous solutions has been investigated through rheological measurements and supported by dynamic light scattering. The copolymer is constituted of a long central poly(2-vinylpyridine) block end-capped by two shorter poly(acrylic acid) blocks, (PAA_{135}−$P2VP_{628}$−PAA_{135}). At pH 3.4 of interest, the copolymer behaves as polyampholyte, bearing positively charged protonated 2VP and negatively charged AA moieties. In aqueous solutions where a physical gel is formed, rheological investigation showed a pronounced thermothickening behavior upon heating to 35 °C, followed by a weak zero-shear viscosity decrease. This unexpected temperature dependence has been interpreted by considering a competition between two antagonistic effects: (i) a remarkable swelling of the macromolecular chain upon heating, mainly due to the excluded-volume effect of the outer PAA blocks, that favors intermolecular interactions between oppositely charged blocks responsible for physical gelation and (ii) the thermal motion of molecules which speeds up the molecular dynamics and tends to weaken the rheological properties. The effect of the macromolecular swelling prevails at low temperatures while the influence of the thermal motion increases continually and predominates at high temperatures.

Introduction

Associative polymers, generally used as rheology modifiers for their thickening properties, are of prime interest in numerous industrial applications.[1,2] Thermoassociative polymers represent a particular class of self-associating materials since their thickening properties are promoted upon heating. Indeed, such polymers contain functional groups as poly(ethylene oxide-*co*-propylene oxide),[3] poly(ethylene oxide),[4] or poly(*N*-isopropylacrylamide) (PNIPAM)[5−8] characterized by a lower critical solution temperature (LCST). From a phenomenological point of view, the specific thermal behavior arises from the progressive formation of a transient network constituted by hydrophilic backbone physically cross-linked via hydrophobic interactions of the thermoresponsive groups at temperatures above their LCST.[5,9,10]

Some multiarm star polymers (or colloidal stars) exhibit thermothickening behavior which differs from that mentioned above.[11−13] These soft materials, bridging the gap between polymer solutions and colloidal suspensions, display a counterintuitive reversible gelation upon heating. This thermothickening behavior, which corresponds to a jamming transition, is attributed to the swelling of dangling polymeric arms when temperature is increased, leading to the gradual interpenetration of the soft spheres. It has been shown experimentally that significant swelling results from the enhancement of the solvent quality passing from θ solvent toward good solvent with increasing temperature. The solvent quality can also be improved by choosing the appropriate solvent for the polymeric arms.

Recently, some of us[14a] have demonstrated for the first time that a double hydrophilic water-soluble polymer, i.e., a triblock copolymer of poly(acrylic acid)−poly(vinylpyridine)−poly(acrylic acid) (PAA−P2VP−PAA), may be self-organized reversibly into two distinct and completely different structures (i.e., from a transient three-dimensional network to compact micelles) by switching the pH of the aqueous media. This interesting and novel behavior was attributed to the nature and the specific architecture of the polymer named asymmetric triblock polyampholyte.[14a]

In the present work, an unexpected and rather complex reversible thermothickening phenomenon exhibited by the same polymeric material is presented. At pH 3.4 of interest in this study, the water-soluble PAA−P2VP−PAA copolymer exhibits a polyampholyte character since the central P2VP block is partially protonated and therefore bears positive charges while a limiting number of negative charges exist in the PAA blocks due to the acrylic acid dissociation. At $T = 25$ °C and above a critical concentration, a previous work has shown that this copolymer forms a transient network through electrostatic interactions between oppositely charged blocks of different chains[14b] which probably is stabilized by hydrogen bonding between the uncharged moieties. Some "topological defects" in the mechanically active network, consisting of nonassociated "dangling ends" and polymeric chains involved in intramolecular associations, have been considered to account for a pronounced shear thickening effect. It has been shown that these "defects" depend on the mechanical history of the material. For example, a sufficient high shear stress induces an intra- to interassociation transition and forces the "dangling ends" to join the mechanically

[†] ICE/HT-FORTH.
[‡] University of Patras.
[§] Institute of Electronic Structure and Laser.
* Corresponding author: Fax +30 2610 997 266; e-mail ct@chemeng.upatras.gr.

10.1021/ma047520p CCC: $30.25
Published on Web 03/03/2005

active network, leading to a significant zero-shear viscosity enhancement after a preshearing. On the basis of this molecular approach, we have extended the previous study by a thorough investigation of the temperature dependence of polyampholyte's rheological behavior in salt-free water. The unexpected thermoresponsiveness of this polymeric material is compared with that observed in other systems mentioned above and discussed in terms of microstructure by using dynamic light scattering.

Experimental Section

Materials. The PAA−P2VP−PAA triblock copolymer was synthesized by anionic polymerization. Details of the synthesis are given elsewere.[14a] The degree of polymerization is 628 for the central P2VP block and 135 for each PAA end-block, having total weight-average molecular weight M_w 8.5 × 10^4 g/mol and molecular polydispersity M_w/M_n = 1.11. The copolymer is water-soluble, and its aqueous solutions give a pH close to 3.4. The net charge of the polyampholyte is positive (the isoelectric point was found at pH 5.5) due to the asymmetric architecture of the macromolecule. Polymer solutions were obtained by dissolving the proper amount of polymer in distilled water, and a resting time of 24 h at room temperature was applied before measurements. All the prepared polymer solutions were clear, showing that no macroscopic phase separation was present in the solutions.

Rheometry. Rheological measurements were carried out using a controlled stress Rheometric Scientific SR 200, equipped with a cone and plate geometry (diameter = 25 mm, cone angle = 5.7°, truncation = 56 μm). The temperature was controlled between 10 and 50 °C with an accuracy of ±0.1 °C by a water bath circulator. All rheological measurements were performed with a 4 wt % polymer solution (c/c^* of about 1.6), for which a physical gel is formed at 25 °C.[14b] After loading, each sample was kept at rest for 5 min before measurements to remove the mechanical history. Viscosity measurements were taken in a steady-state condition. For this purpose, shear stress sweep tests were carried out with an equilibration time of 100 s and a time evolution of the shear rate smaller than 1% per second. To prevent water evaporation, samples were enclosed in a small solvent trap.

Dynamic Light Scattering. Characterization of the polymeric solution as a function of temperature in the dilute regime (c = 0.5 wt %) was achieved via dynamic light scattering. The normalized intensity time correlation function $g^{(2)}(q,t) = \langle I(q,t)I(q,0)\rangle/\langle I(q)\rangle^2$ was measured at various scattering angles and temperatures spanning a time scale from 10^{-7} to 10^3 s. The measurements were performed with a Nd:YAG laser (ADLAS) operating at 532 nm with a stabilized power of 100 mW in an ALV goniometer setup. The polarization conditions of the incident and scattered radiation were controlled by utilizing a set of a Glan and Glan-Thomson polarizers (Halle, Berlin) with an extinction coefficient better than 10^{-7}. The scattered light was analyzed with a full multiple-τ fast digital correlator (ALV-5000/E) with 280 channels. The relaxation of concentration fluctuations in the polymer solution due to the Brownian motion of the polymer was detected at different scattering wave vectors $q = (4\pi n/\lambda)\sin(\theta/2)$, where n is the refractive index of the solvent and θ the scattering angle. The intermediate scattering function, $C(q,t)$, was deduced from $g^{(2)}(q,t)$ by the Siegert relation[15]

$$g^{(2)}(q,t) = 1 + f^*|C(q,t)|^2 \tag{1}$$

where f^* is an instrumental factor related to the coherence area. $C(q,t)$ was analyzed as a weighted sum of independent contributions

$$C(q,t) = \int L(\ln \tau)\exp(-t/\tau)\, d\ln\tau \tag{2}$$

The distribution of relaxation times $L(\ln \tau)$ was obtained by the inverse Laplace transformation (ILT) of $C(q,t)$ using the CONTIN algorithm.[16] The apparent hydrodynamic radii of macromolecules were determined using the Stokes−Einstein relation

$$R_H = \frac{k_B T}{6\pi\eta D} \tag{3}$$

where k_B is the Boltzmann constant, η is the viscosity of the solvent, and D is the diffusion coefficient. The latter was determined by $D = \Gamma/q^2$ at the limit $q = 0$, where Γ is the decay rate of $C(q,t)$.

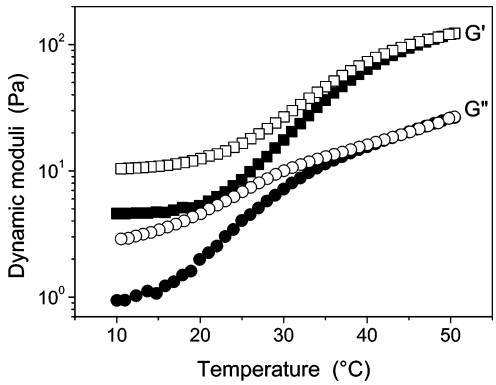

Figure 1. Dynamic temperature ramp for a 4 wt % solution monitored at 1 rad/s with a temperature rate of 0.5 °C/min. Full symbols correspond to data obtained by increasing temperature and open symbols to that obtained by decreasing temperature.

Results and Discussion

Rheology. a. Oscillatory Shear Measurements. Figure 1 depicts the linear viscoelastic response of the 4 wt % polymer solution subjected to an increasing temperature ramp (full symbols) followed by a decreasing temperature ramp (open symbols). Measurements were conducted at a frequency ω = 1 rad/s in a temperature range from 10 to 50 °C with a temperature rate of 0.5 °C/min. It is evident that the polymer solution exhibits a pronounced reversible thermothickening effect. However, both moduli G' and G'' undergo a hysteresis effect over a complete cycle of temperature change. This leads to a partial recovery of their values at the end of the heating/cooling sweep test. This peculiar temperature dependence observed for a nonthermoassociative polymer could be due to a specific thermodynamic process characterized by an intrinsic hysteresis and/or a slow kinetic behavior, at least slower than the experimental time scale. Further experiments were performed to characterize thoroughly this unusual thermoresponsive effect.

We first focus our attention on the behavior of G' and G'' moduli as a function of shear strain. The shear strain dependence of storage modulus G' and loss modulus G'' normalized by their plateau values G'_0 and G''_0 are shown in Figures 2 and 3, respectively, for different temperatures ranging from 18 to 50 °C. Let us stress that the term "plateau values" is used in this paper to qualify the strain-independent (i.e., linear) viscoelastic moduli determined at a fixed frequency. For all temperatures considered, the solution exhibits a linear viscoelastic response below a critical shear strain $\gamma_c \sim 0.3$, where both G' and G'' moduli are independent of shear strain. A further increase in the amplitude of the oscillatory shear strain leads to strain hardening characterized by a pronounced increase in G' followed by an appreciable drop at even higher strains.

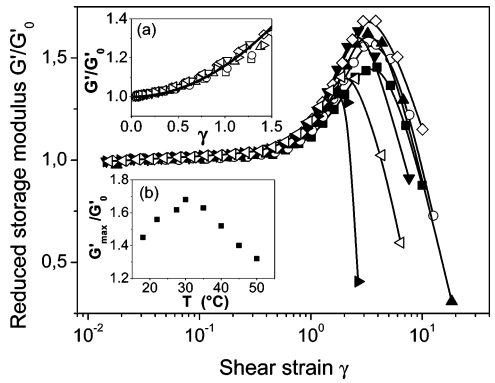

Figure 2. Reduced storage modulus G'/G'_0 of the 4 wt % solution as a function of shear strain γ at $T = 18$ (■), 22 (○), 27.5 (▲), 30 (◇), 35 (▼), 45 (tilted △), and 50 °C (tilted ▲) and $\omega = 3$ rad/s. Inset: (a) Reduced storage modulus G'/G'_0 as a function of shear strain γ. (b) Peak intensity of the reduce storage modulus G'_{max}/G'_0 as a function of temperature. The full line in inset (a) shows a fit of a second-order power series in γ^2.

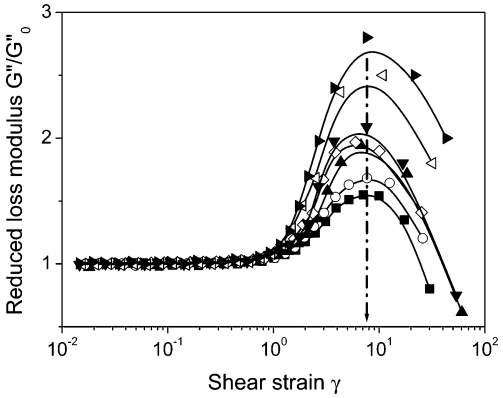

Figure 3. Reduced loss modulus G''/G''_0 of the 4 wt % solution as a function of shear strain γ at $T = 18$ (■), 22 (○), 27.5 (▲), 30 (◇), 35 (▼), 45 (tilted △), and 50 °C (tilted ▲) and $\omega = 3$ rad/s.

From a molecular point of view, the origin of the strain hardening evidenced in G' modulus might be twofold. As proposed in our previous work,[14b] the shear strain at moderated deformations increases the number of intermolecular interactions between adjacent chains, which become part of the stress-conducting network, leading to an enhancement of the storage modulus. This effect results from a modification of the molecular conformation which may induce a second effect. The polymer backbone, adopting a wormlike conformation at rest, can be stretched under large strains, increasing its rigidity, and as a result the solution becomes increasingly stiffer. On the basis of this assumption, Gisler et al.[17] have proposed a model to describe the nonlinear feature of G' as a function of shear strain for colloidal gels which yields

$$G'(\gamma) \propto \sum_{n=0}^{\infty} \frac{1}{(2n+1)!} I_{4n+5} I_{2n+2} \left(\frac{A\gamma}{2}\right)^{2n} \qquad (4)$$

where $I_k = \int_0^{2\pi} \sin^k \theta \, d\theta$ and $A = (1 + d_b)/(d_b - 1)$, d_b being the connectivity or chemical dimension, which characterizes the scaling of the contour length within the cluster. This relation has been tested in Figure 2, inset (a), where all reduced storage moduli G'/G'_0 obtained at different temperatures have been plotted as a function of shear strain. A second-order power series of eq 4, i.e., $n = 0$, 1, 2 with $d_b \approx 2.5$, matches remarkably well the shear strain dependence of the G' modulus up to $\gamma \sim 1.5$, i.e., well above the linear viscoelastic range. This result suggests that the connectivity of the network is self-similar in this lowest range of strain amplitude for all tested temperatures. Moreover, it has to be noted that the strain hardening strength, denoted as G'_{max}/G'_0 and plotted in inset (b) as a function of temperature, increases up to $T \sim 30$ °C where it starts to decrease gradually with increasing temperature. According to the molecular approach of the strain hardening, the increase of G'_{max}/G'_0 upon heating until $T \sim 30$ °C suggests (i) an increase of intermolecular interactions, which leads to an increase of the number of the elastically active chains, and/or (ii) the existence of a more stretched conformation of the polymer backbone. Above $T \sim 30$ °C, the shear strain amplitude denoted as γ_{max}, associated with the maximum in G', decreases sharply upon heating, reflecting a rupture of the transient network at weaker deformations when the temperature is increased. A direct consequence of this effect is the progressive decrease of the strength of the strain hardening of G' above $T \sim 30$ °C. The self-similarity of the network structure observed at low strain amplitude could reflect the predominance of the stretching effect while intermolecular associations may be favored at higher strain amplitudes, leading to a more structured network.

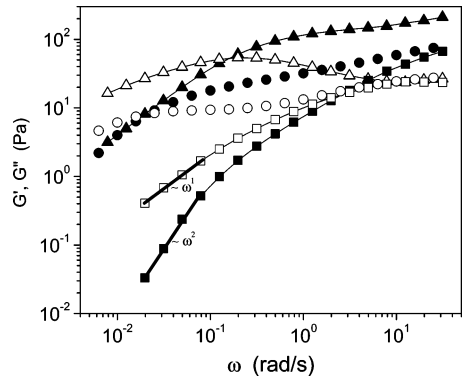

Figure 4. Storage modulus (full symbol) and loss modulus (open symbol) of the 4 wt % solution as a function of frequency at 12.5 (■, □), 25 (●, ○), and 50 °C (▲, △).

As far as the loss modulus G'' is concerned, its strain hardening strength increases continuously with increasing temperature. On a molecular level, the loss modulus reflects generally the effective volume occupied by the transient network. Consequently, the strain hardening of the loss modulus may originate from the extension (stretching) of the polymer coil that results in an increase of the volume occupied by the network. The above arguments might suggest that the length of the polymer coil increases continuously with increasing temperature.

Figure 4 shows the linear viscoelastic behavior of the solution as a function of frequency at $T = 12.5$, 25, and 50 °C. At $T = 12.5$ °C, G' and G'' moduli are respectively proportional to ω^2 and ω^1 at low frequencies, corresponding to the classical terminal zone. At $T = 25$ °C, the G' modulus is significantly higher than the G'' modulus, and both moduli increase in parallel slowly at high frequencies. Such a behavior is characteristic of fractal gel structures, in agreement with the discussion following eq 4. At 50 °C, the linear viscoelastic behavior of the solution is qualitatively similar to that

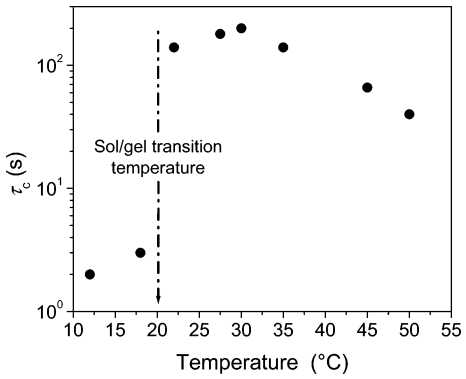

Figure 5. Characteristic time τ_c, corresponding to the inverse of the frequency associated with the $G'-G''$ crossover, as a function of temperature.

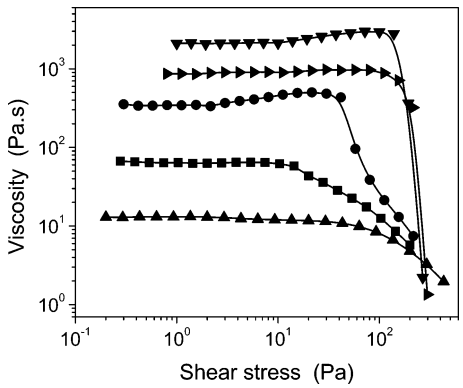

Figure 6. Apparent viscosity of the 4 wt % solution as a function of shear stress at $T = 12.5$ (▲), 18 (■), 22 (●), 35 (▼), and 50 °C (tilted ▲).

obtained at 25 °C, but both moduli are globally enhanced by increasing temperature. Moreover, the $G'-G''$ intersection is observed at a higher characteristic frequency, ω_c, than at 25 °C.

In Figure 5 the characteristic time $\tau_c = 2\pi/\omega_c$ determined at the $G'-G''$ intersection is plotted as a function of temperature. For $T < 20$ °C, the order of magnitude of the characteristic time of about 2 s is in good agreement with that classically encountered for associative polymers for which association/dissociation processes dominate.[18,19] A sudden increase of the characteristic time appears clearly at $T \sim 20$ °C. Such a jump, similar to a characteristic time divergence, resembles a sol/gel transition. Above 30 °C, the characteristic time decreases continuously with increasing temperature. This result shows that the molecular dynamics become faster by increasing temperature above $T \sim 30$ °C, which could be partly attributed to the enhancement of the thermal motion of polymeric molecules. However, the latter cannot justify solely the magnitude of the observed τ_c decrease, and probably other changes of the interactions sensitive to temperature may occur.

b. Steady Shear Measurements. Figure 6 shows the apparent viscosity of the polymer solution as a function of shear stress for temperatures between 12 and 50 °C. Three different temperature regimes can be identified from this figure. Below $T \sim 20$ °C, the flow curves exhibit a Newtonian plateau η_0 at low shear stress followed by a shear thinning above a critical shear stress. In this temperature regime, an increase in temperature induces an increase of the Newtonian viscosity associated with a sharp decrease of the critical shear stress value. This behavior reveals a gradual

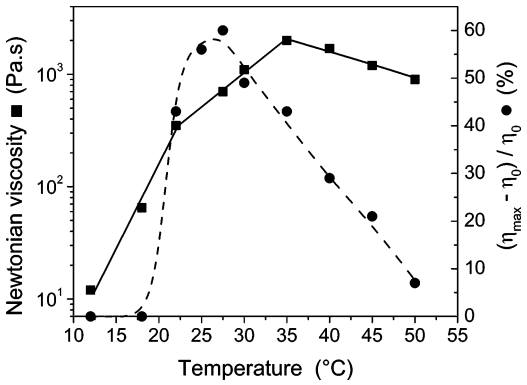

Figure 7. Newtonian viscosity η_0 and intensity of the shear thickening effect $(\eta_{max} - \eta_0)/\eta_0$ expressed in percentage of the Newtonian viscosity of the 4 wt % solution as a function of temperature.

structure formation in the solution upon heating. The viscous behavior changes above the temperature $T \sim 20$ °C that corresponds to the abrupt τ_c enhancement evidenced from viscoelastic measurements. In particular, a shear thickening effect appears just after the linear regime, followed by an abrupt shear thinning. Such discontinuity in the flow curve is generally observed in the viscous response of a physical gel, for which the intermolecular dissociation process prevails beyond the critical shear stress, in the dissociation/association competition. However, this high-temperature regime ($T > 20$ °C) can be divided in two subregimes. Between $T \sim 20$ and 35 °C, the Newtonian viscosity and the critical shear stress still increase with temperature while they both decrease gradually above $T \sim 35$ °C. The temperature dependence of the Newtonian viscosity η_0 and the strength of the shear thickening effect quantified by $(\eta_{max} - \eta_0)/\eta_0$, where η_{max} is the maximum value of the viscosity, are depicted in Figure 7. The Newtonian viscosity profile points out three temperature regimes similar to those observed previously. The temperature at $T \sim 20$ °C marks both a significant reduction of the rate of increase of the Newtonian viscosity upon heating and a sudden increase of the shear-thickening effect. On the contrary, above $T \sim 35$ °C the Newtonian viscosity decreases according to an Arrhenius law

$$\eta_0 \sim \exp(E_a/RT) \tag{5}$$

where the activation energy $E_a \sim 46$ kJ/mol can be considered as the potential barrier to disengage a chain from a junction point. The value of E_a is in the same order of magnitude but slightly lower than that determined for hydrophobically associated HEUR telechelic polymer with similar weight-average molecular weight end-capped by $C_{16}H_{33}O$ hydrophobic groups.[20,21] The thermothinning behavior observed above 35 °C, a classical behavior for complex and/or simple fluids, like most polymer solutions, is due to the gradual increase of the macromolecular thermal motion with increasing temperature which has been previously observed in Figure 5. The increase of the thermal motion might also be probably responsible for the progressive vanishing of the shear-thickening effect.

Dynamic Light Scattering. Figure 8 illustrates representative experimental data, i.e., correlation functions $C(q,t) = \sqrt{(g^{(2)}(q,t)-1)/f^*}$ at a scattering angle $\theta = 90°$ ($q = 0.022$ nm^{-1}) for a dilute, 0.5 wt %, polymer

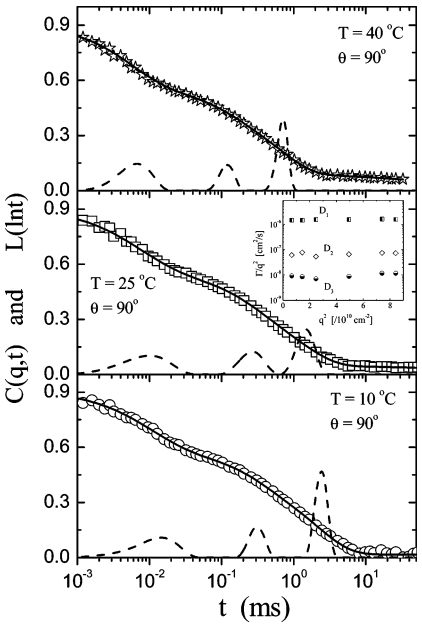

Figure 8. Representative autocorrelation functions, $C(q,t)$, of the 0.5 wt % polymer solution at $\theta = 90$ °C ($q = 0.022$ nm^{-1}) and three temperatures, $T = 10$, 25, and 40 °C. Open symbols stand for the experimental data. Solid lines through the data points represent the best fit results using eq 2. Dashed lines correspond to the distribution of relaxation time, $L(\ln \tau)$, obtained from inverse Laplace transformation. Inset: q dependence of the diffusion coefficient $D = \Gamma/q^2 = 1/q^2\tau$ for the three relaxation modes.

solution ($c/c^* = 0.2$) at three temperatures, as well as the corresponding distributions of relaxation times obtained with the aid of the inverse Laplace transform (ILT) technique (cf. eq 2). The solid line through the experimental points (open symbols) is the best fit curve using eq 2.

At first sight, the correlation functions seem to exhibit a two-step relaxation pattern with well-separated fast and slow modes. Analyzing the experimental data with a double stretched exponential formalism, we found that the fast mode is purely exponential while the slow process is stretched with stretching exponent of about 0.5. This appreciable stretching implies either polydispersity or the existence of species with different sizes. Indeed, the ILT distributions revealed the existence of two kinds of particles whose hydrodynamic radii, as calculated by means of eq 3, correspond to aggregates.

All these three modes are found to exhibit diffusive character as evidenced from the q independence of the diffusion coefficient $D = \Gamma/q^2$ shown in the inset of Figure 8. The decay rates Γ were calculated from the maxima of the ILT distributions. The fast mode corresponding to a "particle" size of about 1 nm should be associated with ion diffusion observed in pure P2VP at the same conditions.[22] The other two modes correspond to sizes of about 26 and 170 nm, respectively. The temperature dependence of the hydrodynamic radii of the two slow modes is shown in Figure 9. Since the radius of gyration, R_g, of single chains in salt-free solution is estimated to be 11 nm,[22] the two slow modes reflect the presence of small associates (with 2−3 associated chains) and large clusters, respectively. Direct observation by atomic force microscopy confirms that in this concentration regime the majority of single chains are participating in small assemblies and larger loose clusters.[23]

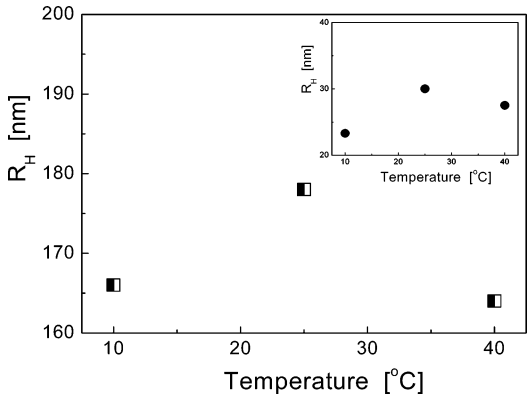

Figure 9. Temperature dependence of the hydrodynamic radii, R_H, of the slowest relaxation modes exhibited in the intensity autocorrelation function of the 0.5 wt % polymer solution.

The temperature dependence of the hydrodynamic radii exhibits an interesting behavior. With increasing temperature in the range 10−25 °C the hydrodynamic radii of the two slow modes, small associates and clusters, grow from 23.3 to 30 nm for the former and from 166 to 178 nm for the latter. This effect is consistent with the viscosity data which show also a drastic increase in the same temperature range. Increasing further the temperature to 40 °C, we observe a modest speed-up of the diffusion associated with these two modes or equivalently a decrease in the related hydrodynamic radii; this fact again reflects viscosity changes above 25 °C. It is obvious that both of the apparent hydrodynamic radii increase with temperature and reach a maximum value at $T = 25$ °C. At low temperatures ($T < 15$ °C), the PAA outer blocks adopt a compact coil conformation since they are close to theta conditions (UCST).[24] On the other hand, the main P2VP central block is partially protonated and therefore exhibits a more stretched conformation.[25] In such a situation, intermolecular association through electrostatic interactions and/or hydrogen bonding are prevented, and the viscosity of the system is low. The swelling of the polymer chain observed upon heating should be mainly attributed to the expansion of the PAA coils (excluded-volume effect) at both ends of the macromolecule giving rise to the development of the intermolecular interactions and thus to an increase of the elastically active chains which contributes to the storage modulus enhancement. It is worth mentioning that molecular dynamics simulations have predicted a reversible swelling of neutral random polyampholyte backbone characterized by a hysteresis when the long-range Coulomb force and short-range attraction force cooperate.[26,27] Such specific predisposition for polyampholytes could explain the hysteresis observed in dynamic moduli of solutions subjected to a temperature cycle.

Dynamic light scattering results support the analysis obtained from the rheological results, which suggests a more effective intermolecular association of the polymer upon heating. The molecular swelling of the PAA outer blocks favors intermolecular interactions mainly between the oppositely charged blocks,[14] leading to the formation of a physical gel. However, most of the PAA units and about 70% of P2VP units (pH 3.4) are uncharged, and hydrogen bonding between the different moieties should exist which stabilize the association.[28] Simultaneously, the thermal motion increases and its

effect becomes predominant above $T \sim 35$ °C, for which the molecular expansion reaches a certain limit. The thermal motion prevalence at high temperature is related with the significant decrease of the characteristic time determined by dynamic rheology and the weakening of the shear-thickening and the strain-hardening effects. However, the magnitude of this decrease cannot be ascribed only to thermal motion, suggesting a weak alteration of the structure which is evident by light scattering. The observed decrease of the size of the clusters could be attributed to the weakening of the hydrogen-bonding contribution on the intermolecular association since the H-bonds are not favored upon heating.[29]

Concluding Remarks

In this study, a rich and rather unexpected thermosensitivity of an asymmetric triblock polyampholyte of the type $PAA_{135}-P2VP_{628}-PAA_{135}$ in salt-free aqueous solutions has been presented through rheological measurements and supported by dynamic light scattering. With increasing temperature, the whole set of rheological data demonstrate a sol/gel like transition, 2 orders of magnitude viscosity enhancement, while the rheological properties of the gel above $T \sim 35$ °C exhibit Arrhenius behavior. This peculiar thermal response results from the competition between the significant swelling of the PAA outer blocks, which favors intermolecular interactions responsible for the pronounced thermothickening behavior and the thermal motion, which weaken the rheological properties of the polymer solution by speeding up the molecular dynamics. The partial expansion of the polymer chains upon heating is a consequence of the enhancement of the solvent quality. The results reported in this study emphasize the serious impact of the solvent quality in the rheological behavior of soluble polymers, which is frequently overlooked or taken into account less seriously.

The novelty of this thermoresponsive behavior arises from the fact that none of the polymeric components of the copolymer exhibit LCST, which was the only reason known so far to induce the thermothickening effect in associative polymers. On the contrary, the outer PAA blocks exhibit UCST. In such a case, coil expansion occurs upon heating, allowing the intermolecular interactions mainly among oppositely charged moieties to develop, leading eventually to the formation of an infinite transient network.

Acknowledgment. We thank Prof. Dimitris Vlassopoulos, Prof. Thierry Aubry, and Prof. G. Staikos for fruitful discussions and comments about this work, which has been performed with the financial support of the European Community under Grant HPMD-CT2000-00054-02.

References and Notes

(1) Glass, J. E. *Polymers in Aqueous Media: Performance through Associations*; Advances in Chemistry Series 223; American Chemical Society: Washington, DC, 1989.
(2) Shalaby, S. W.; McCormick, C. L.; Buttler, G. B. *Water Soluble Polymers. Synthesis, Solution Properties and Applications*; ACS Symposium Series 467; American Chemical Society: Washington, DC, 1991.
(3) Vos, S.; Möller, M.; Viscchер, K.; Mijnlieff, P. F. *Polymer* **1994**, *35*, 2644.
(4) Hourdet, D.; L'Alloret, F.; Audebert, R. *Polymer* **1994**, *35*, 2624. (b) Hourdet, D.; L'Alloret, F.; Durand, A.; Lafuma, F.; Audebert, R.; Cotton, J.-P. *Macromolecules* **1998**, *31*, 5323.
(5) Bokias, G.; Hourdet, D.; Iliopoulos, I.; Staikos, G.; Audebert, R. *Macromolecules* **1997**, *30*, 8293.
(6) Durand, A.; Hourdet, D. *Polymer* **1999**, *40*, 4941.
(7) Bokias, G.; Mylonas, Y.; Staikos, G.; Bumbu, G. G.; Vasile, C. *Macromolecules* **2001**, *34*, 4958.
(8) Aubry, T.; Bossard, F.; Staikos, G.; Bokias, G. *J. Rheol.* **2003**, *47*, 577.
(9) Sarrazin-Cartalas, A.; Iliopoulos, I.; Audebert, R.; Olsson, U. *Langmuir* **1994**, *10*, 1421.
(10) Loyen, K.; Iliopoulos, I.; Audebert, R.; Olsson, U. *Langmuir* **1995**, *11*, 1053.
(11) Kapnistos, M.; Vlassopoulos, D.; Fytas, G.; Mortensen, K.; Fleischer, G.; Roovers, J. *Phys. Rev. Lett.* **2000**, *85*, 4072.
(12) Stiakakis, E.; Vlassopoulos, D.; Loppinet, B.; Roovers, J.; Meier, G. *Phys. Rev. E* **2002**, *66*, 051804.
(13) Stiakakis, E.; Vlassopoulos, D.; Roovers, J. *Langmuir* **2003**, *19*, 6645.
(14) Sfika, V.; Tsitsilianis, C. *Macromolecules* **2003**, *36*, 4983. (b) Bossard, F.; Sfika, V.; Tsitsilianis, C. *Macromolecules* **2004**, *37*, 3899.
(15) Berne, B. J.; Pecora, R. *Dynamic Light Scattering with Application to Chemistry, Biology, and Physics*; Wiley Nescience: New York, 1976. (b) Schulz-DuBoir, E. O. In *Photon Correlation Techniques in Fluid Mechanics*; Schulz-DuBoir, E. O., Ed.; Springer-Verlag: Berlin, 1983; p 15.
(16) Provencer, S. W. *Comput. Phys. Commun.* **1982**, *27*, 213.
(17) Gisler, T.; Ball, R. C.; Weitz, D. A. *Phys. Rev. Lett.* **1999**, *82*, 1064.
(18) Aubry, T.; Moan, M. *J. Rheol.* **1994**, *38*, 1681.
(19) Leibler, L.; Rubinstein, M.; Colby, R. H. *Macromolecules* **1991**, *24*, 4701.
(20) Annable, T.; Buscall, R.; Ettelai, R.; Whittlestone, D. *J. Rheol.* **1993**, *37*, 695.
(21) Tam, K. C.; Jenkins, R. D.; Winnik, M. A.; Bassett, D. R. *Macromolecules* **1998**, *31*, 4149.
(22) Beer, M.; Schmidt, M.; Muthukumar, M. *Macromolecules* **1997**, *30*, 8375.
(23) Tsitsilianis, C.; Stavrouli, N.; Gorodyska, A.; Kiriy, A.; Minko, S.; Stamm, M., to be published.
(24) Silberberg, A.; Eliassaf, J.; Katsalski, A. *J. Polym. Sci.* **1957**, *23*, 259.
(25) Minko, S.; Kiriy, A.; Gorodyska, G.; Stamm, M. *J. Am. Chem. Soc.* **2002**, *124*, 3218. (b) Gorodyska, A.; Kiriy, A.; Minko, S.; Tsitsilianis, C.; Stamm, M. *Nano Lett.* **2003**, *3*, 365−368.
(26) Tanaka, M.; Grosberg, A. Yu; Pende, V. S.; Tanaka, T. *Phys. Rev. E* **1997**, *56*, 5798.
(27) Tanaka, M.; Grosberg, A. Yu; Tanaka, T. *Langmuir* **1999**, *15*, 4052.
(28) Giebeler, E.; Stadler, R. *Macromol. Chem. Phys.* **1997**, *198*, 3815.
(29) Aoki, T.; Kawashima, M.; Katono, H.; Sanui, K.; Ogata, N.; Okano, T.; Sakurai, Y. *Macromolecules* **1994**, *27*, 947.

MA047520P